2011

Nonlocal instability analysis of FCC bulk and (100) surfaces under uniaxial stretching

Geng Yun
University of Colorado, Boulder, CO

Penghui Cao
Boston University, Boston, MA

Jonathan Zimmerman
Sandia National Laboratories, Livermore, CA

Terry Delph
Lehigh University, Bethlehem, PA

Harold Park
Boston University, Boston, MA

International Journal of Solids and Structures 48 (2011) 3406–3416

Contents lists available at SciVerse ScienceDirect

International Journal of Solids and Structures

journal homepage: www.elsevier.com/locate/ijsolstr

Nonlocal instability analysis of FCC bulk and (100) surfaces under uniaxial stretching

Geng Yun [a], Penghui Cao [d], Jonathan A. Zimmerman [c], Terry J. Delph [b], Harold S. Park [d,*]

[a] Department of Mechanical Engineering, University of Colorado, Boulder, CO 80309, United States
[b] Department of Mechanical Engineering and Mechanics, Lehigh University, Bethlehem, PA 18015, United States
[c] Mechanics of Materials Department, Sandia National Laboratories, Livermore, CA 94550, United States
[d] Department of Mechanical Engineering, Boston University, Boston, MA 02215, United States

ARTICLE INFO

Article history:
Received 11 April 2011
Received in revised form 15 July 2011
Available online 23 August 2011

Keywords:
Nonlocal instability criteria
Surface instability
Defect participation volume

ABSTRACT

The objective of this paper is to examine the instability characteristics of both a bulk FCC crystal and a (100) surface of an FCC crystal under uniaxial stretching along a ⟨100⟩ direction using an atomistic-based nonlocal instability criterion. By comparison to benchmark atomistic simulations, we demonstrate that for both the FCC bulk and (100) surface, about 5000–10,000 atoms are required in order to obtain an accurate converged value for the instability strain and a converged instability mode. The instability modes are fundamentally different at the surface as compared to the bulk, but in both cases a strong dependence of the instability mode on the number of atoms that are allowed to participate in the instability process is observed. In addition, the nonlocal instability criterion enables us to determine the total number of atoms, and thus the total volume occupied by these atoms, that participate in the defect nucleation process for both cases. We find that this defect participation volume converges as the number of atoms increases for both the bulk and surface, and that the defect participation volume of the surface is smaller than that of the bulk. Overall, the present results demonstrate both the necessity and utility of nonlocal instability criteria in predicting instability and subsequent failure of both bulk and surface-dominated nanomaterials.

1. Introduction

Since Hadamard (1903), the notion of instability in continuous solids has been studied by many authors (Hill, 1962; Stroh, 1962; Rudnicki and Rice, 1975; Rice, 1976; Hill and Milstein, 1977; Gao, 1996). In these continuum mechanics-based formulations, as originated by Hill (1962), a small perturbation is applied to an infinite body of a solid, and a material stability analysis is performed to determine whether the perturbation grows unboundedly with time. If it does, the material is considered to be unstable; if it does not, the material is considered to be stable (Belytschko et al., 2002). Furthermore, the material stability analysis depends upon the state of deformation in the material through the determinant of an acoustical tensor, which depends upon both the current state of stress and stiffness in the material. We note that other researchers have extended these concepts to analyze, in a continuum fashion, the stability of surfaces attached to an infinite half space (Srolovitz, 1989; Suo et al., 1992).

Recently, nanomaterials have been extensively studied, and found to exhibit superior mechanical properties (Park et al., 2009), with the particularly salient property of having a strength that has been found to approach a significant fraction of the ideal strength (Zhu and Li, 2010). Because of this, and the related interest in connecting macroscale instability to atomic-scale processes, there has been a burst of activity applying continuum mechanics concepts to study instability in nanomaterials. There have typically been two approaches to this class of problems. The first involves the determination of crystal elastic constants directly from an underlying interatomic potential, which are then directly utilized for a material stability analysis (Milstein and Huang, 1978; Alber et al., 1992; Wang et al., 1993, 1995; Kitamura et al., 2004; Lu and Zhang, 2006). Other researchers have made a multiscale link between interatomic potentials and continuum mechanics, typically using the Cauchy–Born hypothesis, such that finite element calculations of atomic scale instability can be performed at both zero (Li et al., 2002; Vliet et al., 2003; Zhu et al., 2004; Pacheco and Batra, 2008) and finite temperature (Xiao and Yang, 2007).

One key issue that has recently drawn attention is the fact that instabilities at the atomic scale, for example dislocation nucleation, tend to involve the collective motion of a group of atoms, rather than originating with an individual atom. If this is the case, then such instabilities have an inherently nonlocal character. This point was first noted by Miller and Rodney (2008), who demonstrated

* Corresponding author.
E-mail address: parkhs@bu.edu (H.S. Park).

0020-7683/$ - see front matter © 2011 Elsevier Ltd. All rights reserved.
doi:10.1016/j.ijsolstr.2011.08.009

using atomistic simulations of nanoindentation that single atom-based instability criteria, which have dominated previous nanoscale instability research (Li et al., 2002; Lu and Zhang, 2006; Pacheco and Batra, 2008; Zhu et al., 2004; Vliet et al., 2003), are unable to capture the nonlocal nature of nanoscale instability initiation or defect nucleation. The importance of nonlocality in capturing nanoscale instability nucleation was further addressed by Delph et al. (2009), Delph and Zimmerman (2010), who developed a nonlocal instability criterion called the Wallace criterion, and demonstrated for a variety of situations that a collection of atoms on the order of a few hundred was necessary to accurately predict the instability nucleation. We note that the Wallace criterion thus takes an intermediate point of view in terms of computational expense between the single-atom-based instability measures (Li et al., 2002; Vliet et al., 2003; Zhu et al., 2004; Lu and Zhang, 2006; Pacheco and Batra, 2008), and those which require the evaluation of the Hessian matrix for the entire collection of atoms (Kitamura et al., 2004; Lu and Zhang, 2006), which can be computationally prohibitive. Justification for such an intermediate point of view has also been given by Dmitriev et al. (2004), who found that prior to lattice instabilities, or bond breaking, spatial localization of the unstable mode does occur.

One important issue that has not been addressed, and that we focus upon in the present work, is the issue of nonlocal instability or defect nucleation from the surfaces of nanomaterials. Surface instabilities are critical in nanomaterials because recent theoretical (Gall et al., 2004; Park et al., 2006, 2009) and experimental (Zheng et al., 2010) studies have demonstrated that defects in nanomaterials tend to nucleate at the surfaces rather than within the nanomaterial bulk. Therefore, because surface atoms have fewer bonding neighbors than atoms within the bulk, they exist at a less stable energetic configuration, and are also more likely to be driven to instability under applied loading. We are aware of two atomistic-based studies, the first being that of Dmitriev et al. (2005), who studied the atomistic stability of elastic half-planes and determined that surfaces are less stable than their bulk counterparts. There are, however, substantial differences between that work and the present work. The major distinctions are that first, Dmitriev et al. (2005) considered a 2D half-space, and not a fully 3D system by using a single periodic cell of the sample, which inherently limits the effects of nonlocality. Secondly, their instability criteria is based upon the eigenvalues of the force constant matrix, whereas the present work is based upon determining the eigenvalues of a Hessian which is related to the energetic stability of a given configuration of atoms. The second is the more recent work of Umeno et al. (2010) who studied the effects of free surfaces on lattice instabilities in copper thin films. While a nonlocal instability measure was utilized in that work, their analysis considered the entire volume of the atomic system and thus all atomistic degrees of freedom, rather than a subset of the total volume. Because of this, the effect of the size of the nonlocal region on the instability mode and strain and a comparison of the instability modes that are observed at surfaces as compared to the FCC bulk were not performed.

Therefore, there are two objectives of the present work. The first is to perform a comprehensive study of the effects of nonlocality on the instabilities that occur in both a bulk FCC crystal and a (100) surface of an FCC crystal that is subjected to uniaxial stretching along a ⟨100⟩ direction. We contrast the influence of nonlocality on the surface instability mechanisms that are observed to that observed in a bulk FCC crystal under the same uniaxial stretching. The second objective is to utilize the nonlocal instability criterion to determine the volume of atoms, which we term the defect participation volume, that is necessary to nucleate a defect in both the bulk FCC crystal and the (100) surface. Again, contrasts are drawn between the defect participation volumes that are found for both the FCC bulk and (100) surface.

2. Nonlocal Wallace criterion

The ideas underlying the Wallace criterion (Wallace, 1972) have been elucidated in recent work (Delph et al., 2009; Delph and Zimmerman, 2010). In the Wallace approach, we consider a region Ω containing a total of N atoms. These atoms are free to move in an arbitrary fashion, apart from any external restraints upon the atomic motion. The atoms surrounding the region Ω, however, are assumed to remain motionless, including those atoms, M in number, that interact with the interior atoms and are contained within an annulus surrounding Ω. Fig. 1 shows a sketch of this situation, both for the case of the bulk and the surface analysis. Implicit in this scenario is the idea that atomic-scale instabilities may be adequately characterized by the motion of the atoms within Ω, and that the motion of the atoms outside this region may be neglected. We will subsequently present detailed results in support of this idea.

For all numerical results in the present work, the shape of the volume Ω containing the N atoms was taken to be spherical or hemispherical though we emphasize that there is no restriction on the shape of the volume Ω. For example, a rectangular prism was

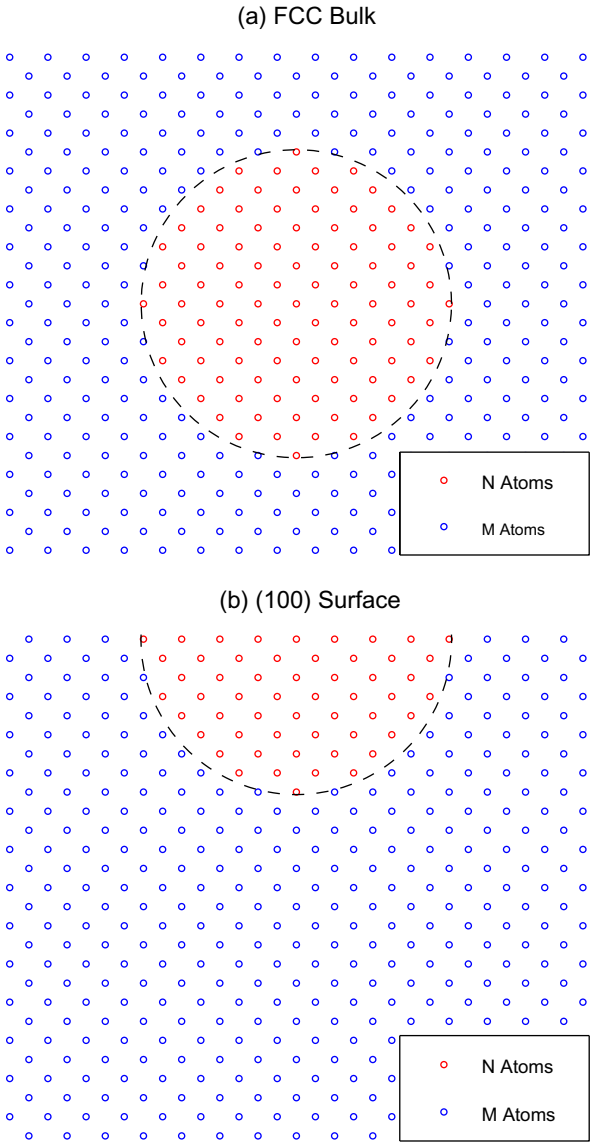

Fig. 1. (a) Spherical region Ω in a bulk FCC crystal that contains the N atoms that participate in the failure process surrounded by M atoms; (b) hemispheral region used to analyze (100) surface instabilities that contains the N atoms that participate in the failure process surrounded by M atoms.

considered by Delph et al. (2009) to study the initiation of crack propagation in an FCC crystal. We note that one factor in considering a spherical participation volume, particularly with respect to quasicontinuum (Tadmor et al., 1996) or Cauchy–Born like models is that the unit cells utilized in those models are based upon a spherical truncation due to the cut-off radius of the interatomic potential.

For a pair potential, the equilibrium potential energy Φ_0 of the N atoms can be written as

$$\Phi_0 = \sum_{\alpha=1}^{N-1} \sum_{\beta=\alpha+1}^{N} V(R^{\alpha\beta^2}) + \sum_{\alpha=1}^{N} \sum_{\gamma=1}^{M} V(R^{\alpha\gamma^2}), \tag{1}$$

where $R^{\alpha\beta^2}$ is the square of the distance between atoms α and β, V is the interatomic potential, the first term on the right hand side of (1) represents interactions between pairs of atoms contained within Ω (N–N interactions), and the second term on the right hand side of (1) represents interactions between interior and exterior atoms (N–M interactions). Performing a Taylor expansion around the initial equilibrium state with respect to R, we can express to first order the change in energy as a quadratic form

$$\Phi - \Phi_0 = \sum_{k=1}^{3N} \sum_{l=1}^{3N} A_{kl} v_k v_l, \tag{2}$$

where the v_i represent arbitrary infinitesimal displacements of the N group of atoms. The linear terms in this expansion vanish by virtue of the fact that the initial state is taken to be an equilibrium state. The Hessian matrix A_{kl} can be determined analytically as a function of the first and second derivatives of a given interatomic potential (Delph et al., 2009; Delph and Zimmerman, 2010).

The basic idea underlying the Wallace criterion is that, for a stable deformation increment from an arbitrary equilibrium state Φ_0 to a new state Φ, the change in energy $\Phi - \Phi_0$ will be positive. Equivalently, this can be formalized by stating that the eigenvalues of the matrix A_{kl} remain positive. However, for an unstable deformation increment, the change in energy $\Phi - \Phi_0$ will be negative, i.e. the new state has a lower energy than the previous equilibrium configuration, which manifests itself physically at the atomic scale by the nucleation of a defect such as a dislocation followed by the relaxation of the dislocation and the surrounding crystal. This transition to a lower energy configuration thus corresponds to the emergence of a negative eigenvalue of the Hessian matrix A_{kl}. We note that the Hessian A_{kl} of the present work is a factor of two times the Hessian defined in several previous works, for example that of Miller and Rodney (2008), Dmitriev et al. (2005); we refer the reader to the detailed discussion in Delph et al. (2009).

In summary, the Wallace criterion exhibits at least four desirable features as compared to previous local, or single-atom instability criteria. First, the criteria is nonlocal, rather than local; we will demonstrate in the numerical examples the importance of this in capturing the instability strains and modes. Second, the stability of the atomistic system can be easily assessed by examining the lowest eigenvalue of the Hessian A_{kl}. Third, because the number of atoms N that are needed to capture the nonlocal instability occurrence are typically about 5000–10,000, the computational cost in calculating the lowest eigenvalue of such a $3N \times 3N$ matrix is quite moderate. Fourth, the eigenvectors v in (2) reflect the motion of the N atoms as the instability occurs, and thus offer insights into the instability mode. We note, however, that the Wallace criterion is, at present, restricted to zero temperature and includes no thermal effects.

3. Numerical results

We performed atomistic simulations of uniaxial stretch along $\langle 100 \rangle$ directions in a bulk FCC crystal using the atomistic simulation code LAMMPS (LAMMPS, 2006; Plimpton, 1995). The simulations were all performed under zero-temperature quasistatic conditions; thus, the simulations were of the molecular mechanics (i.e. energy minimization, or molecular statics) type rather than finite temperature molecular dynamics. The crystals were deformed in uniaxial stretch along the x-direction using the deformation gradient

$$F_{tens} = \begin{pmatrix} \lambda & 0 & 0 \\ 0 & 1 & 0 \\ 0 & 0 & 1 \end{pmatrix}, \tag{3}$$

where λ is the stretch ratio in the $\langle 100 \rangle$ direction.

In the present work, we utilize the smooth Lennard–Jones (LJ) potential of Eerden et al. (1992), which takes the form

$$\Phi(r) = 4.569\epsilon \left(\left(\frac{\sigma}{r}\right)^{12} - \left(\frac{\sigma}{r}\right)^{6} \right) \exp\left(\frac{0.25\sigma}{r - 2.5\sigma}\right), \tag{4}$$

to model the interatomic interactions. The LJ parameters, as taken from Eerden et al. (1992) are: $\sigma = 3.3$ Å and $\epsilon/k_b = 119.8$ K, where k_b is the Boltzmann constant, which leads to an FCC lattice parameter of 5.12 Å. This particular form of the LJ potential was chosen because it smoothly truncates to zero at the cutoff radius $r_c = 8.25$ Å, along with both its first and second derivatives. The smoothness of the first and second derivatives is desired because both derivatives are required to calculate the Hessian A_{kl} in (2). Because this is a simple pair potential, the results we obtain subsequently should be interpreted as being qualitative in nature, rather than quantitative, and thus do not represent the behavior of any particular material.

The bulk atomistic simulations were performed as follows. First, the bulk FCC crystal was deformed according to the deformation gradient in (3), at which point an additional random perturbation on the order of 0.01 Å was applied to the resulting atomic positions of the N atoms. The positions of the N atoms were then allowed to relax to energy minimizing positions that were close to, but not identical to, those specified by the deformation gradient. The positions of the surrounding M atoms, on the other hand, were strictly specified by the applied deformation gradient. The perturbation had the effect of introducing a slight randomness into the atomic positions, which facilitated the instability by breaking the symmetry of the crystal. For the bulk FCC crystal, sufficient M atoms were provided such that the N atoms had a complete bonding environment.

The surface stretching results were performed slightly differently than for the bulk FCC crystal. Specifically, a full LAMMPS simulation, with no constraints upon the motion of any atom, was run, and a stretch value close to the point of instability identified. This was done to capture the effects of surface relaxation, which were found to be critical to accurately predicting the surface instability mode. A grouping of N atoms contained within a region Ω was then identified, along with the surrounding interacting M atoms. For stretching past this point, the motion of all atoms exterior to Ω, including the M atoms, was taken to be strictly specified by the applied deformation gradient, and only the interior group of N atoms allowed to relax. We note that, due to the inherent symmetry-breaking effect of the free surface, no additional random perturbation was applied to the atomic positions in order to obtain the instability stretch.

For both the bulk and surface cases, instability in the LAMMPS simulations was signaled by a sudden drop in the global potential energy with increasing stretch. Fig. 2 illustrates this process for the bulk FCC crystal with $N = 459$. Values of N up to around 10,000 were considered to examine the effects of the degree of nonlocality upon the instability stretch and mode. Specifically, for the largest bulk case that was considered, there were 9909 N atoms, which

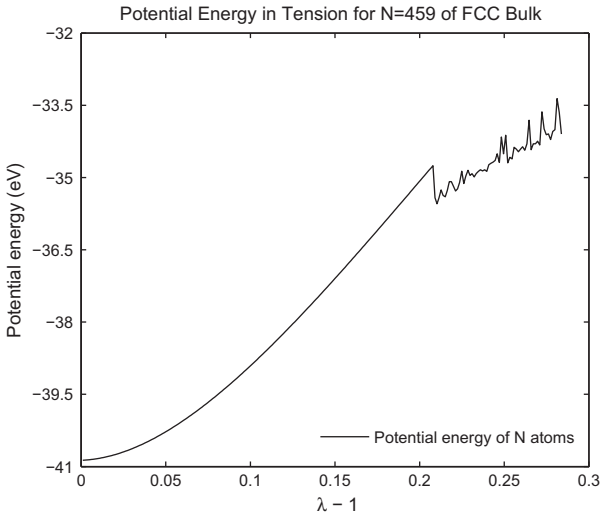

Fig. 2. Potential energy vs. stretch curves for $N = 459$ for bulk FCC crystal.

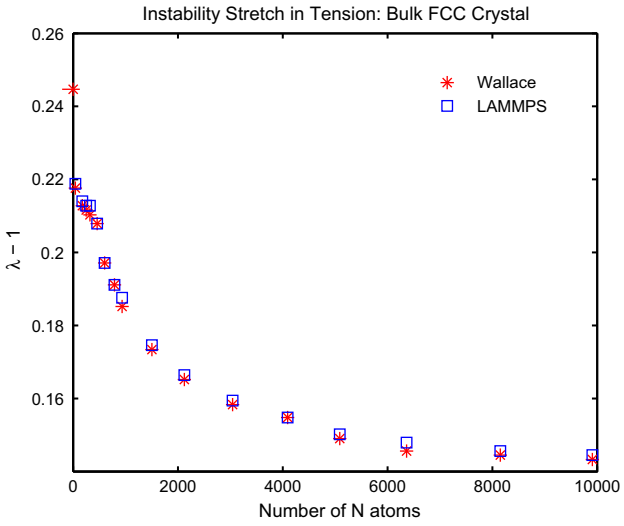

Fig. 3. Instability stretch comparison for a bulk FCC crystal under uniaxial stretch along a ⟨100⟩ direction as calculated using direct atomistic simulation (LAMMPS), and the nonlocal Wallace criterion.

were surrounded by 32,683 *M* atoms, while for the largest surface case that was considered, there were 8674 *N* atoms, which were surrounded by 27,830 *M* atoms.

Once equilibrium, energy-minimizing positions were found using LAMMPS, the atomic positions of the *N* and surrounding *M* atoms taken from these simulations were used to calculate the Hessian matrix A_{kl} resulting from the Wallace criterion. The lowest eigenvalue of the Hessian was then extracted and its sign examined. If the eigenvalue was positive, then the LAMMPS simulation was rerun to a larger value of stretch. This procedure was repeated until a stretched configuration resulted for which the lowest eigenvalue of the Hessian matrix became negative.

3.1. Uniaxial stretching of the bulk FCC crystal

We first examine the performance of the Wallace criterion in predicting the onset of instability in a bulk FCC crystal stretched uniaxially along a ⟨100⟩ direction. Fig. 3 shows the critical stretch as a function of the number of atoms *N* considered in the context of the Wallace criterion. It can be seen that the critical stretch at instability as derived from the Wallace criterion and the LAMMPS calculations are in excellent agreement with each other for a given value of *N*. There are several noteworthy features in Fig. 3 that merit further discussion. First, we note that there is a significant drop in instability stretch that occurs as more atoms *N* are allowed to participate in the instability nucleation. It can be seen that the instability stretch is about 0.245 if a single atom, i.e. $N = 1$, is allowed to participate. However, the instability stretch decreases and appears to converge to a value of about 0.14 once *N* approaches about 10,000, which suggests the importance of nonlocality for predicting instability in bulk crystals. Second, we note that independent LAMMPS simulations for an unperturbed perfect FCC crystal using 23,328 atoms yielded an instability stretch of about 0.1319, which is in excellent agreement with the asymptotic value shown in Fig. 3. Third, the agreement between the Wallace prediction and the direct atomistic simulation for the instability strain is found to be quite good, with the largest deviation being about 1.5% when $N = 6363$.

An important attribute of the Wallace criterion is its ability to predict the initial motion of the atoms during the nucleation of the defect. By construction, the eigenvector of the Wallace Hessian matrix A_{kl} corresponding to a particular eigenvalue represents the atomic displacements associated with this mode, in particular the instability mode corresponding to the lowest eigenvalue as it approaches zero. This feature can yield useful information as to the nature of the defect. To illustrate this point, we first stretched the crystal directly to the point of instability, and then monitored the variation in system potential energy during the LAMMPS convergence process. Fig. 4 shows an example of this. It can be seen that, at a certain point in the energy minimization process, the potential energy drops sharply, indicating the nucleation of a defect. The point before the potential energy drop occurs is marked by a square in Fig. 4. The atomic coordinates corresponding to this point were used to calculate the Wallace Hessian matrix A_{kl}, whose eigenvectors yield the predicted initial motion of the atoms at the point of instability. Approximate atomic motions at the instability point were also computed from LAMMPS as the difference between the atomic positions at the iteration at which the potential energy drop begins, and those at the next iteration output step, which we term the displacement vector in the present work.

The eigenvectors from the Wallace calculation and the displacement vectors from the benchmark fully atomistic (LAMMPS)

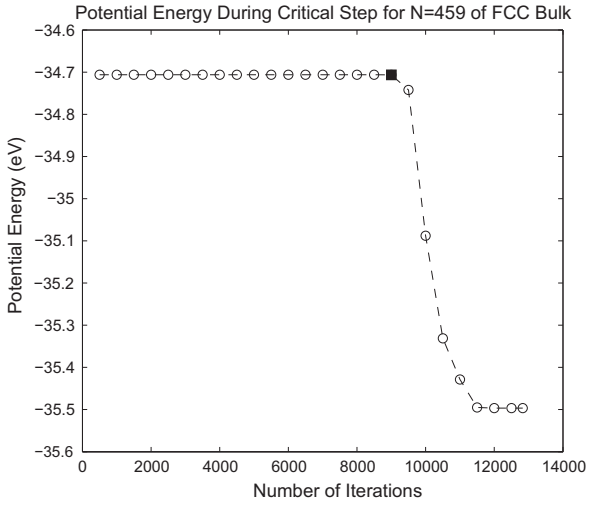

Fig. 4. Potential energy for the $N = 459$ atoms versus the number of iterations during the energy minimization process for the critical (instability) step for tension of the bulk FCC crystal, where the exact point of instability is marked by the square around iteration 9000.

calculation are shown in Fig. 5. Fig. 5(a) shows a 2D view of the displacement vectors and eigenvectors on the *yz* plane at $x = 0$ in Fig. 5(a), which represents the center plane of the *N* atoms and is also orthogonal to the tensile loading (*x*) direction. A fully 3D comparison is shown in Fig. 5(b). Fig. 5 clearly demonstrates that the initial motion of the atoms during nucleation of the instability is predicted similarly by both the Wallace criterion and the fully atomistic simulation, which is encouraging given the complex motion of the atoms that is observed in Fig. 5. In addition, while the instability mode is somewhat unclear from the 2D plot in Fig. 5(a), the fully 3D comparison in Fig. 5(b) clearly suggests a tensile cavitation or separation-type failure mode.

We should also emphasize here that, while the Wallace criterion accurately predicts the initial motion of the atoms at the point of instability, it does not predict the final atomic configuration that occurs at the end of the instability step. This is because the Wallace criterion is essentially a saddle point criterion, where the motion of the atoms at the saddle (instability) point does not necessarily coincide with their final configuration as they descend down the potential energy well.

We close the section on the stretching of a bulk FCC crystal by noting that, just as the instability stretch converges with increasing *N*, so does the initial motion of the atoms at the point of instability. This is demonstrated by comparing the eigenvectors as obtained using the Wallace analysis for $N = 1505$ and $N = 5089$ in Fig. 6, which shows a 2D cross sectional view of the *xy* plane; we note that similar conclusions can be drawn by looking at 2D cross sectional views of the *xz* and *yz* planes.

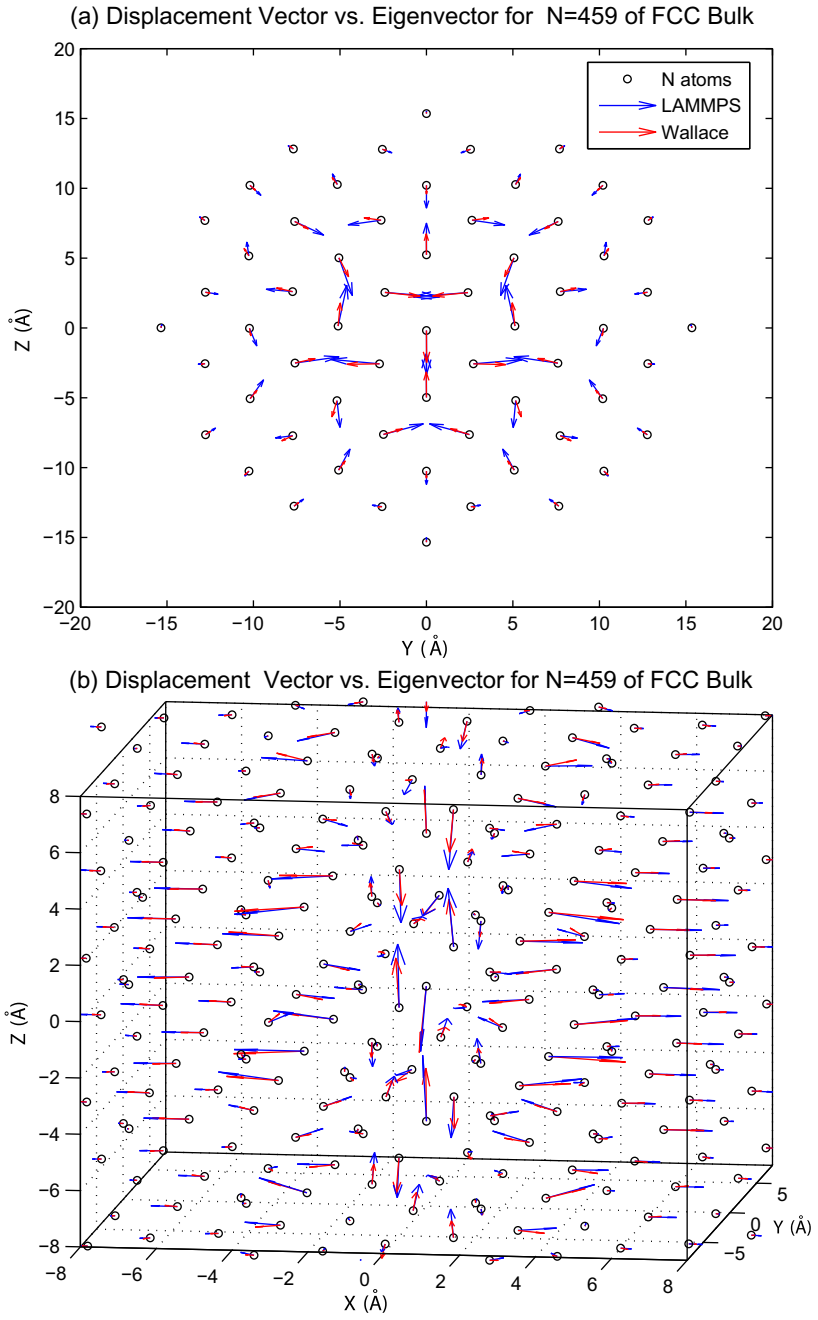

Fig. 5. Comparison of eigenvectors as calculated from Wallace formulation and displacement vector from fully atomistic simulation stretching a bulk FCC crystal along a ⟨100⟩ direction at onset of instability depicted in Fig. (4) for $N = 459$ as shown in both (a) 2D view of the *yz* plane at $x = 0$, and (b) fully 3D plot.

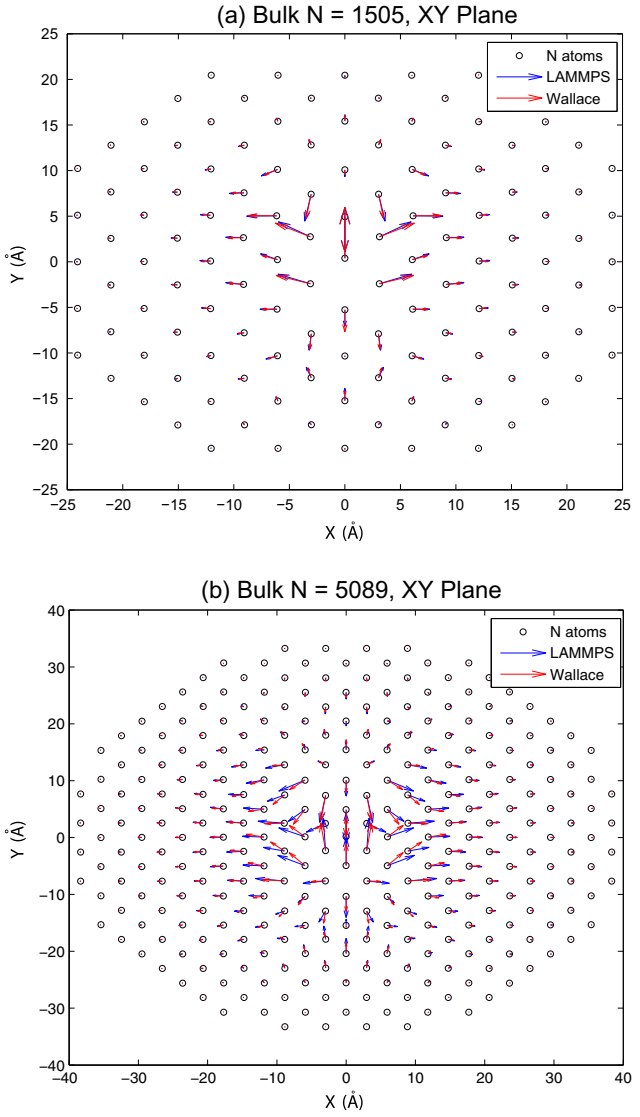

Fig. 6. Comparison of Wallace eigenvectors and LAMMPS displacement vectors on the *xy* plane for uniaxial stretching along a ⟨100⟩ direction for a bulk FCC crystal using (a) $N = 1505$ atoms, and (b) $N = 5089$ atoms.

As can be seen, the instability modes are largely similar between $N = 1505$, and $N = 5089$. Specifically, the *xy* plane in Fig. 6, which is parallel to the loading (x) direction, shows modes of failure that are tensile in nature, and suggest a subsequent failure mode of tensile separation or cavitation. Also interesting is that as N is increased, the number of atoms that participate in the instability motion appears to remain essentially constant; in other words, the atoms near the boundary of N when $N = 5089$ do not contribute to the instability motion. This fact, in conjunction with the converging value for instability strain seen in Fig. 3, strongly suggests that there are a fixed number of atoms N (with N being much larger than one but smaller than 10,000) that are required to accurately capture tensile stretch-driven defect nucleation and initiation in bulk FCC crystals. We will address this point later in the discussion portion of the manuscript.

3.2. Stretching in the plane of a (100) FCC surface

Having discussed the bulk tension results, we now present the results for the stability of a (100) FCC surface subject to uniaxial stretching in the plane along a ⟨100⟩ direction. Comparisons are made with the bulk results to illustrate the differences in the instability behavior of the (100) surface as compared to the corresponding bulk material.

The variation of instability stretch with N is shown in Fig. 7. As was the case with the bulk stability behavior shown in Fig. 3, the instability stretch for the surface decreases rather substantially with increasing N before finally reaching an asymptotic value of about $\lambda - 1 = 0.12$ at a value of around $N = 9000$. This asymptotic value is in excellent agreement with the instability stretch found from a LAMMPS analysis in which all 16,000 atoms in the ensemble were allowed to move in accordance with the energy minimization algorithm, which gave a corresponding value of 0.116. The fact that the surface instability stretch is somewhat smaller than the bulk value is not unexpected, due to the reduced coordination experienced by the surface atoms as compared to their bulk counterparts. In all cases, it can be seen that the LAMMPS simulations in which only N atoms are allowed to participate in the energy minimization process yield instability predictions that are in excellent agreement with those from the Wallace criterion.

The eigenvectors obtained from the Wallace criterion likewise demonstrate convergence with increasing N. Figs. 8 and 9 show the atomic displacement vectors derived from LAMMPS and the Wallace eigenvalues for values of $N = 1626$ and 5441, respectively. The similarities between the results for the two values of N are quite apparent. We note that the largest amplitude motion of the atoms occurs at or near the surface, indicating a surface instability. In particular, a cratering-type of defect initiation is observed, in which some atoms at the surface displace inwards towards the bulk, while pushing other nearby atoms outward towards the surface. Finally, as was the case in the bulk simulations previously discussed, we find that as N is increased between Figs. 8 and 9, the number of atoms that participate in the instability process does not appear to increase significantly. We address this point for the bulk and surface in the next section.

3.3. FCC bulk and (100) surface defect initiation and participation volumes

We now quantify an important point made previously, namely that as the number of atoms N increases for stretching of both the

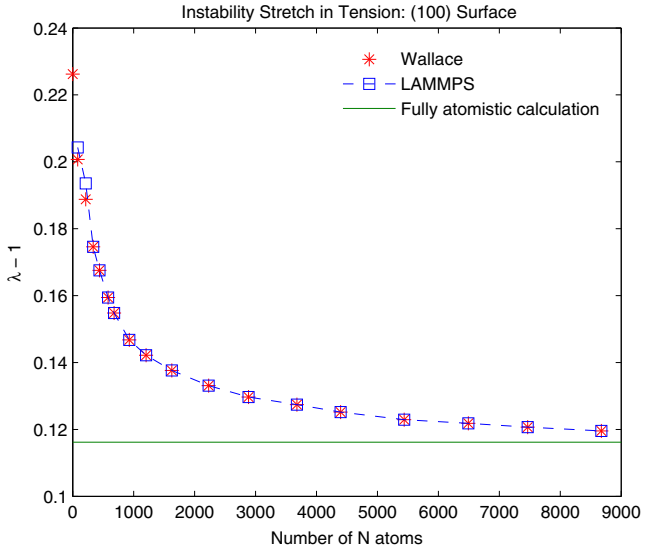

Fig. 7. Instability stretch comparison for the (100) surface of an FCC crystal under uniaxial stretch along a ⟨100⟩ direction as calculated using direct atomistic simulation (LAMMPS), the nonlocal Wallace criterion, and a thin film that is periodic in the plane with a free (100) surface (fully atomistic calculation).

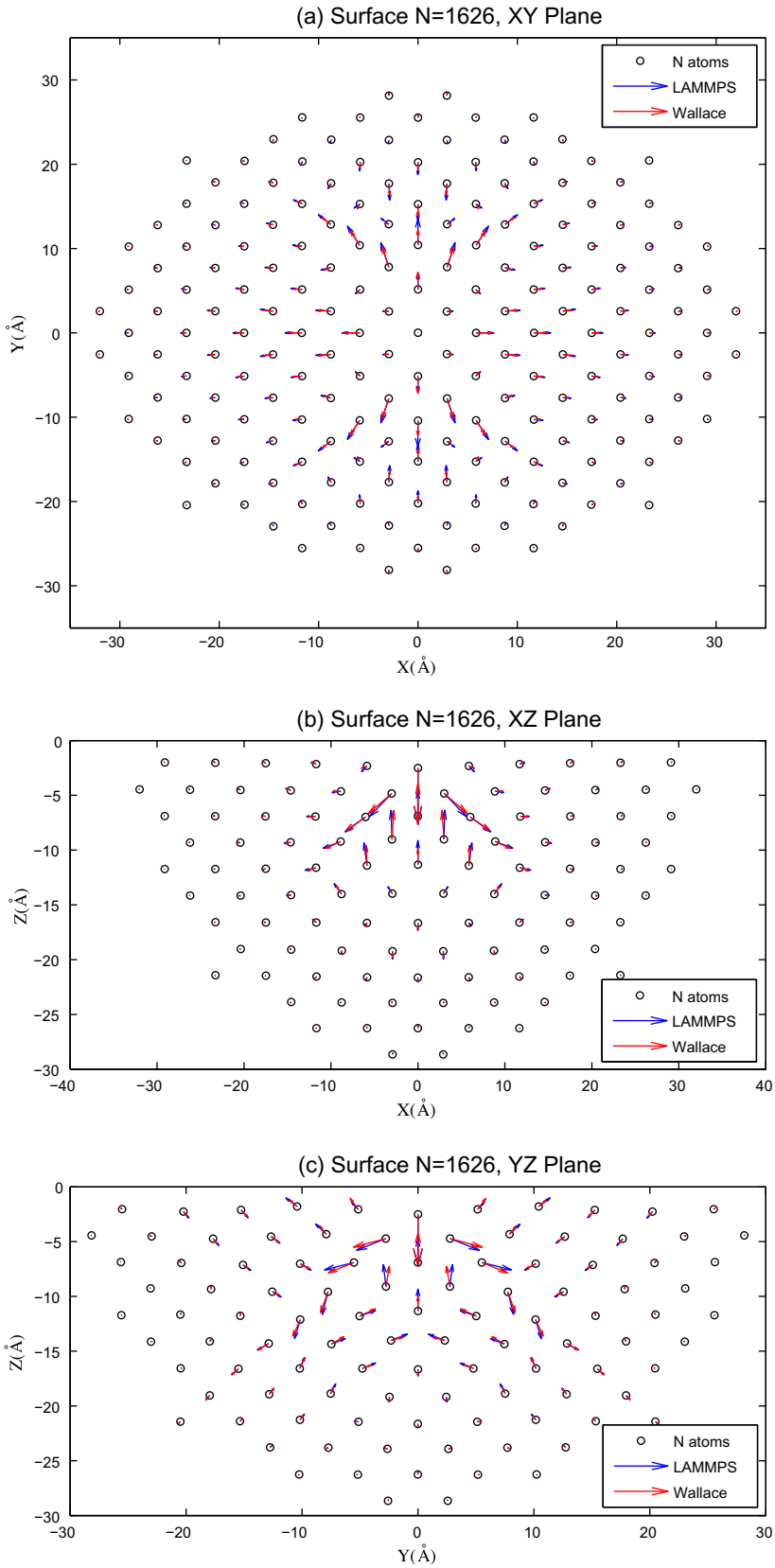

Fig. 8. Comparison of eigenvectors as calculated from Wallace formulation and displacement vector from fully atomistic simulation at onset of instability as shown for (a) *xy*, (b) *xz* and (c) *yz* planes for the (100) surface with $N = 1626$.

FCC bulk and the (100) surface, the number of atoms that show large displacements does not increase appreciably. To investigate this point in more detail, we define two volumes of interest. The first volume, which we term the *defect participation volume*, is intended to serve as a measure of the volume of the subset of atoms within N that are actively participating in the defect nucleation

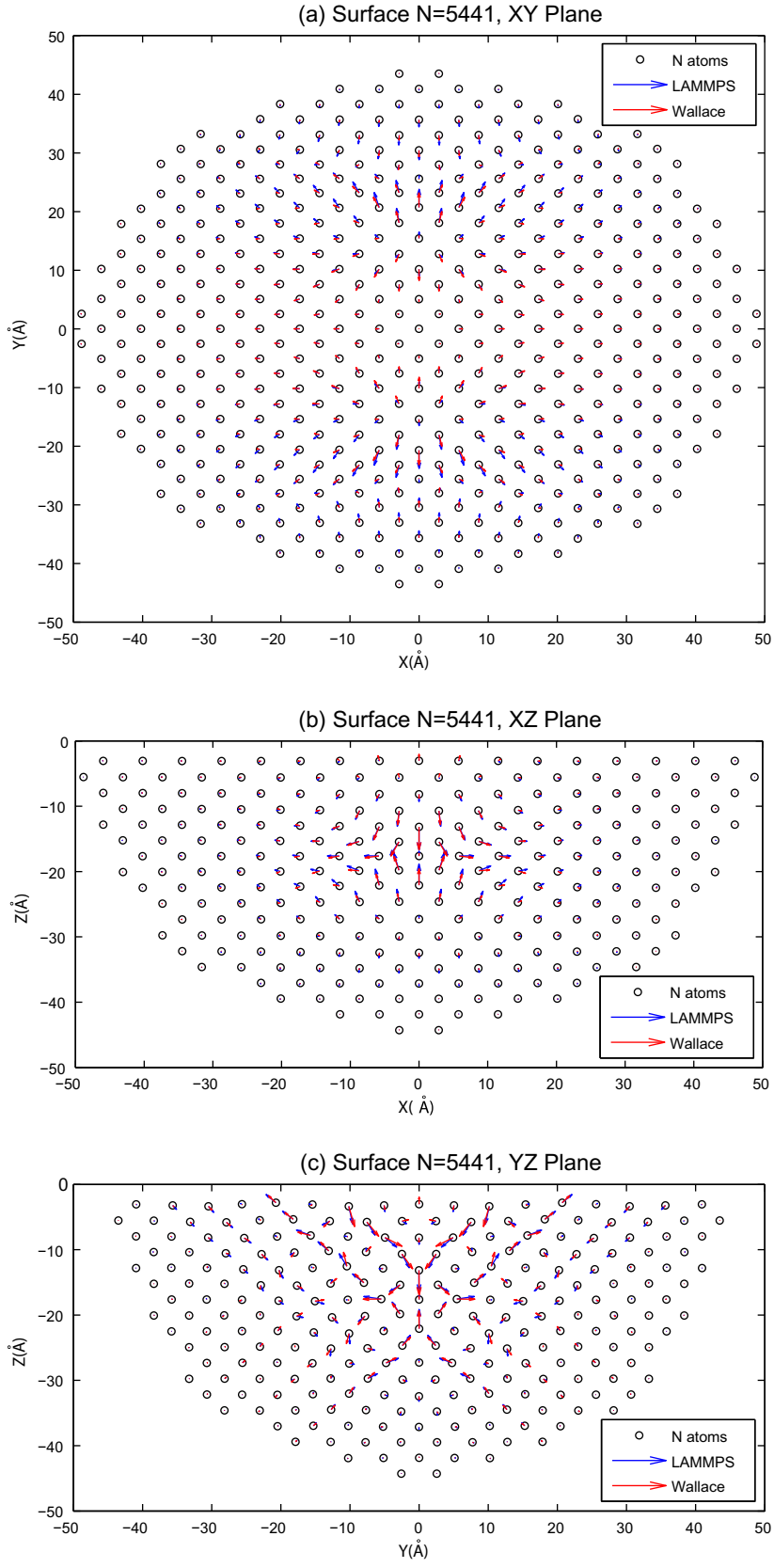

Fig. 9. Comparison of eigenvectors as calculated from Wallace formulation and displacement vector from fully atomistic simulation at onset of instability as shown for (a) *xy*, (b) *xz* and (c) *yz* planes for the (100) surface with $N = 5441$.

process. We defined an atom to be "active" in the instability process if its eigenvector magnitude at the point of instability was greater than a certain percentage of the largest atomic eigenvector magnitude; a threshold of 10% of the largest eigenvector magnitude were chosen for the present work. The defect participation volume was then calculated as the volume occupied by the number

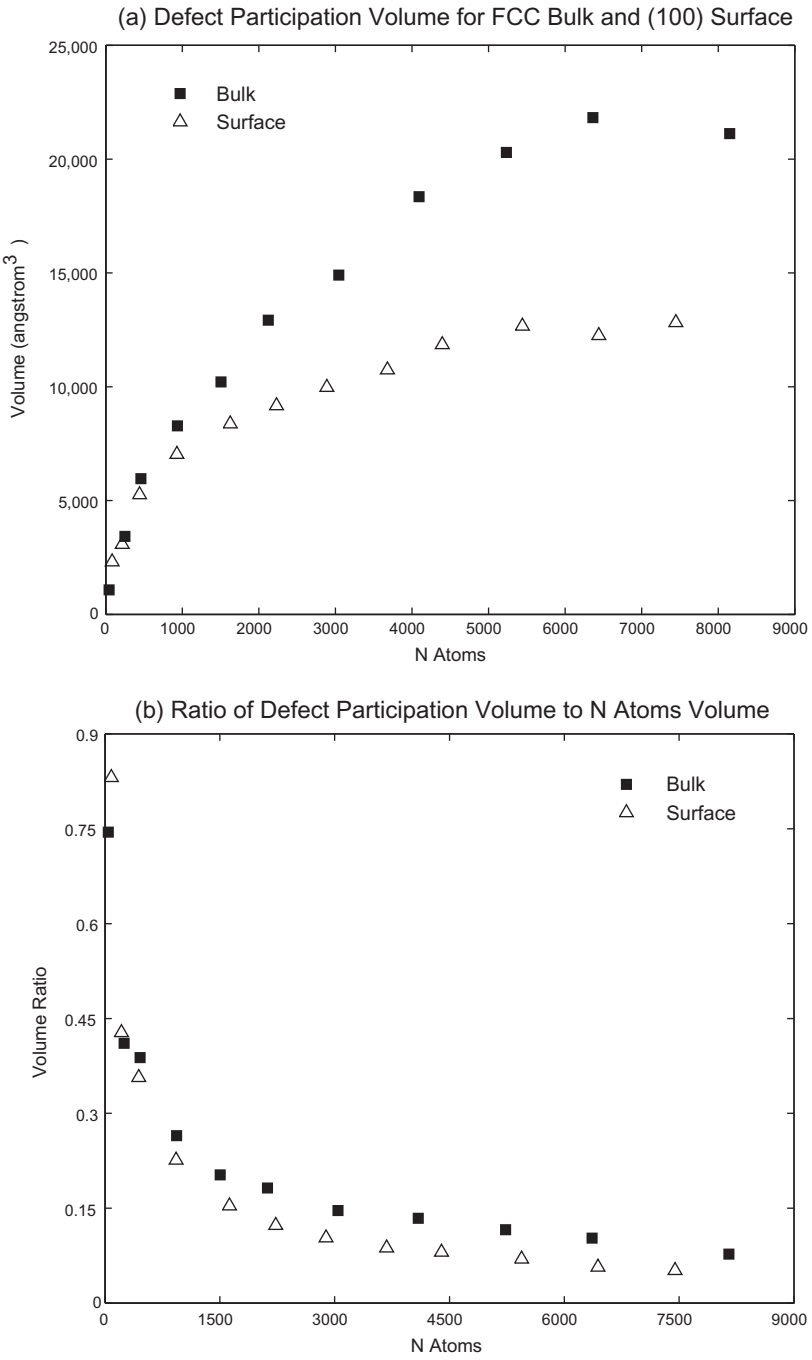

Fig. 10. (a) Defect participation volume and (b) defect participation volume ratio for uniaxial stretching along a ⟨100⟩ direction for both a bulk FCC crystal and a (100) surface.

of atoms whose eigenvector magnitude at the point of instability exceeded the threshold value multiplied by the atomic volume of each atom.

The second volume of interest we define is the *defect initiation volume*, where the defect initiation volume is defined to be the total volume occupied by the N atoms in the undeformed configuration. The reasons for defining two distinct volumes will be made clear in the upcoming discussion. Finally, we also define a defect participation volume ratio, which was calculated as the ratio between the defect participation volume and the defect initiation volume. We note that our choice of the threshold value as 10% of the largest eigenvector magnitude does not impact the trends observed; we found that the defect participation volume decreased for both the bulk and (100) surface as the threshold value increased, as did the defect participation volume ratio.

Before presenting our results, we should note that our definition of defect initiation and participation volumes differ from the definition of activation volume previously presented by Mason et al. (2006), Zhu et al. (2008). In the Zhu et al. (2008) work, the activation volume was defined to be the derivative of activation free energy with respect to stress, i.e. $\Omega(\sigma,T) = -\partial Q/\partial\sigma|_T$, where Ω is the activation volume and Q is the activation free energy. The activation free energy was then found by conducting specialized transition-state-type atomistic simulations based upon the nudged elastic band method that enabled them to calculate the minimum energy pathway between a specified state of stress and the point of

instability. The present definition of defect participation volume is simpler in nature, in that it gives a direct measure of the volume of atoms that are active participants in the instability nucleation process.

Fig. 10(a) shows the impact of the degree of nonlocality on the defect participation volume for both the FCC bulk and (100) surface, while Fig. 10(b) shows the impact of the degree of nonlocality on the defect participation volume ratio. Fig. 10(a) shows that the defect participation volumes for both the bulk and (100) surface converge towards an upper-bound value as N increases, while Fig. 10(b) shows that the defect participation volume ratio converges towards a value under 10% as N increases for both the FCC bulk and (100) surface. As was the case with the trend demonstrated in the plots of instability stretch vs. N, both the defect participation volume and the defect participation ratio seem to approach constant values as N increases. Both of these results are in accordance with the previous discussion surrounding both the results for the FCC bulk in Figs. 5 and 6, and the results for the (100) surface in Figs. 8 and 9. Overall, these results clearly suggest that as the value of N increases, a smaller percentage of atoms in the assemblage experience large motions at the point of instability. Furthermore, our studies suggest that defect initiation due to tensile loading at a (100) surface requires about 50% of the number of atoms as does defect initiation due to tensile loading within the FCC bulk.

Fig. 10(b), in conjunction with the asymptotic trends shown in Figs. 3 and 7, indicates that it may be possible to define a volume containing the minimum value of N atoms necessary to accurately capture the defect initiation, with the atoms outside this volume playing little or no role in the defect nucleation process. This volume we call the defect initiation volume. In the present case, from Fig. 3, this appears to be a volume containing approximately 6000 atoms, corresponding to a volume of about 200,877 $Å^3$; this value ($N = 6000$ atoms) is also valid for the (100) surface case, as seen in Fig. 7. This example also makes clear why two separate volume definitions are needed. Even though it is not evident that the low motion atoms contribute to the instability, it is apparent that their inclusion is necessary in order that the Wallace criterion yield accurate results.

4. Conclusions

We have utilized a nonlocal atomistic-based instability criteria to study the stability of both a bulk FCC crystal and a (100) surface of an FCC crystal that are subject to uniaxial stretching along a ⟨100⟩ direction. Specifically, we have demonstrated that a minimum-sized domain of analysis is required for a conservative estimate of instability prediction in both the bulk and at the surfaces of FCC nanomaterials. The method is not restricted to instability modes related to localized defects, though it certainly can be used in such cases. It can also be applied to instability mechanisms that involve the concerted motion of many atoms.

The key findings are that: (1) A nonlocal criterion, comprising on the order of 5000–10,000 atoms, is required in order to obtained converged values for both the instability strain and initial instability mode for both the FCC bulk and (100) surface. (2) Due to the fact that the surface instability modes originate at or near the (100) free surface, the converged surface instability modes are qualitatively different than those observed for the bulk FCC crystal. (3) Overall, the results indicate that the nonlocal Wallace criterion is able to predict not only the point of instability, but also the initial motion of the atoms at instability for both bulk and surface as compared to benchmark atomistic calculations. (4) The defect participation volume for both the bulk FCC crystal and the (100) surface were found to converge to an upper bound value as N increased, which implies that a finite number of atoms is required to initiate defect nucleation under uniaxial stretch. (5) The defect participation volume for the surface was found to be about 50% smaller than that of the bulk.

Future developments of the Wallace criteria will focus upon investigating temperature effects on the instability strains and instability modes for both the FCC bulk and {100} surface. Preliminary work is currently underway utilizing ideas rooted in transition state theory, similar to that recently done by Zhu et al. (2008), Ryu et al. (2011).

Finally, we close by noting that our analysis shows that a multiscale method that uses the Cauchy–Born (Tadmor et al., 1996; Zhu et al., 2004; Vliet et al., 2003), or surface Cauchy–Born (Park and Klein, 2007; Park and Klein, 2008) models to study defect initiation in nanomaterials would need to incorporate an underlying atomic lattice of about 5000–10,000 atoms at each finite element integration point in order for it to accurate reproduce predictions of tensile stretching-induced instability strains and modes as compared to purely atomistic simulations. However, even with such a requirement, such an approach could be computationally viable.

Acknowledgements

GY acknowledges support from the University of Colorado, while PC acknowledges the support of a Deans Fellowship from Boston University. HSP also acknowledges NSF grant CMMI 0750395 in support of this research. Sandia National Laboratories is a multi-program laboratory managed and operated by Sandia Corporation, a wholly owned subsidiary of Lockheed Martin Corporation, for the U.S. Department of Energy's National Nuclear Security Administration under contract DE-AC04-94AL85000.

References

Alber, I., Bassani, J.L., Khantha, M., Vitek, V., Wang, G.J., 1992. Grain boundaries as heterogeneous systems: atomic and continuum elastic properties. Philosophical Transactions of the Royal Society of London A 39, 555–586.
Belytschko, T., Liu, W.K., Moran, B., 2002. Nonlinear Finite Elements for Continua and Structures. John Wiley and Sons.
Delph, T.J., Zimmerman, J.A., 2010. Prediction of instabilities at the atomic scale. Modelling and Simulation in Materials Science and Engineering 18, 045008.
Delph, T.J., Zimmerman, J.A., Rickman, J.M., Kunz, J.M., 2009. A local instability criterion for solid-state defects. Journal of the Mechanics and Physics of Solids 57, 67–75.
Dmitriev, S.V., Li, J., Yoshikawa, N., Tanaka, Y., Kagawa, Y., Kitamura, T., Yip, S., 2004. Breaking Atomic Bonds Through Vibrational Mode Localization. Defect and Diffusion Forum. Trans Tech Publications, pp. 49–60.
Dmitriev, S.V., Kitamura, T., Li, J., Umeno, Y., Yashiro, K., Yoshikawa, N., 2005. Near-surface lattice instability in 2D fiber and half-space. Acta Materialia 53, 1215–1224.
Eerden, J.P.V.D., Knops, H.J.F., Roos, A., 1992. Monte carlo study of the shear modulus at the surface of a Lennard–Jones crystal. Journal of Chemical Physics 96, 714–720.
Gall, K., Diao, J., Dunn, M.L., 2004. The strength of gold nanowires. Nano Letters 4, 2431–2436.
Gao, H., 1996. A theory of local limiting speed in dynamic fracture. Journal of the Mechanics and Physics of Solids 44, 1453–1474.
Hadamard, J., 1903. Leçons sur la propagation des ondes et les equations de l'hydrodynamique. Paris.
Hill, R., 1962. Acceleration waves in solids. Journal of the Mechanics and Physics of Solids 10, 1–16.
Hill, R., Milstein, F., 1977. Principles of stability analysis of ideal crystals. Physical Review B 15, 3087–3096.
Kitamura, T., Umeno, Y., Tsuji, N., 2004. Analytical evaluation of unstable deformation criterion of atomic structure and its application to nanostructure. Computational Materials Science 29, 499–510.
LAMMPS, 2006. <http://www.cs.sandia.gov/~sjplimp/lammps.html>.
Li, J., Vliet, K.J.V., Zhu, T., Yip, S., Suresh, S., 2002. Atomistic mechanisms governing elastic limit and incipient plasticity in crystals. Nature 418, 302–306.
Lu, J., Zhang, L., 2006. An atomistic instability condition and applications. Journal of Mechanics of Materials and Structures 1, 633–648.
Mason, J.K., Lund, A.C., Schuh, C.A., 2006. Determining the activation energy and volume for the onset of plasticity during nanoindentation. Physical Review B 73, 054102.

Miller, R.E., Rodney, D., 2008. On the nonlocal nature of dislocation nucleation during nano-indentation. Journal of the Mechanics and Physics of Solids 56, 1203–1223.

Milstein, F., Huang, K., 1978. Theory of the response of an fcc crystal to [110] uniaxial loading. Physical Review B 18, 2529–2541.

Pacheco, A.A., Batra, R.C., 2008. Instabilities in shear and simple shear deformations of gold crystals. Journal of the Mechanics and Physics of Solids 56, 3116–3143.

Park, H.S., Klein, P.A., 2007. Surface Cauchy–Born analysis of surface stress effects on metallic nanowires. Physical Review B 75, 085408.

Park, H.S., Klein, P.A., 2008. Surface stress effects on the resonant properties of metal nanowires: the importance of finite deformation kinematics and the impact of the residual surface stress. Journal of the Mechanics and Physics of Solids 56, 3144–3166.

Park, H.S., Gall, K., Zimmerman, J.A., 2006. Deformation of FCC nanowires by twinning and slip. Journal of the Mechanics and Physics of Solids 54, 1862–1881.

Park, H.S., Cai, W., Espinosa, H.D., Huang, H., 2009. Mechanics of crystalline nanowires. MRS Bulletin 34, 178–183.

Plimpton, S.J., 1995. Fast parallel algorithms for short-range molecular dynamics. Journal of Computational Physics 117, 1–19.

Rice, J.R., 1976. The localization of plastic deformation. In: Proceedings of the 14th IUTAM Congress, pp. 207–220.

Rudnicki, J.W., Rice, J.R., 1975. Conditions for localization of deformation in pressure-sensitive dilatant materials. Journal of the Mechanics and Physics of Solids 23, 371–394.

Ryu, S., Kang, K., Cai, W., 2011. Entropic effect on the rate of dislocation nucleation. Proceedings of the National Academy of Science 108, 5174–5178.

Srolovitz, D.J., 1989. On the stability of surfaces of stressed solids. Acta Metallurgica 37, 621–625.

Stroh, A.N., 1962. Steady state problems in anisotropic elasticity. Journal of Mathematics and Physics 41, 77–103.

Suo, Z., Ortiz, M., Needleman, A., 1992. Stability of solids with interfaces. Journal of the Mechanics and Physics of Solids 40, 613–640.

Tadmor, E., Ortiz, M., Phillips, R., 1996. Quasicontinuum analysis of defects in solids. Philosophical Magazine A 73, 1529–1563.

Umeno, Y., Shimada, T., Kitamura, T., 2010. Dislocation nucleation in a thin Cu film from molecular dynamics simulations: instability activation by thermal fluctuations. Physical Review B 82, 104108.

Vliet, K.J.V., Li, J., Zhu, T., Yip, S., Suresh, S., 2003. Quantifying the early stages of plasticity through nanoscale experiments and simulations. Physical Review B 67, 104105.

Wallace, D., 1972. Thermodynamics of Crystals. Wiley, New York, NY.

Wang, J., Yip, S., Phillpot, S.R., Wolf, D., 1993. Crystal instabilities at finite strain. Physical Review Letters 71, 4182–4185.

Wang, J., Li, J., Yip, S., Phillpot, S.R., Wolf, D., 1995. Mechanical instabilities of homogeneous crystals. Physical Review B 52, 12627–12635.

Xiao, S., Yang, W., 2007. A temperature-related homogenization technique and its implementation in the meshfree particle method for nanoscale simulations. International Journal for Numerical Methods in Engineering 69, 2099–2125.

Zheng, H., Cao, A., Weinberger, C.R., Huang, J.Y., Du, K., Wang, J., Ma, Y., Xia, Y., Mao, S.X., 2010. Discrete plasticity in sub-10-nm-sized gold crystals. Nature Communications 1, 144.

Zhu, T., Li, J., 2010. Ultra-strength materials. Progress in Materials Science 55, 710–757.

Zhu, T., Li, J., Vliet, K.J.V., Ogata, S., Yip, S., Suresh, S., 2004. Predictive modeling of nanoindentation-induced homogeneous dislocation nucleation in copper. Journal of the Mechanics and Physics of Solids 52, 691–724.

Zhu, T., Li, J., Samanta, A., Leach, A., Gall, K., 2008. Temperature and strain-rate dependence of surface dislocation nucleation. Physical Review Letters 100, 025502.